

**This is a self-archived version of an original article. This version may differ from the original in pagination and typographic details.**

**Author(s):** Wisniewski, J.; Urban, W.; Czerwinski, M.; Kurpeta, J.; Plochocki, A.; Pomorski, M.; Rzaca-Urban, T.; Sieja, K.; Canete, L.; Eronen, T.; Geldhof, S.; Jokinen, A.; Kankainen, A.; Moore, I. D.; Nesterenko, D. A.; Penttilä, H.; Pohjalainen, I.; Rinta-Antila, S.; de Roubin, A.; Vilén, M.

**Title:** Excited states in  $^{87}\text{Br}$  populated in  $\beta$  decay of  $^{87}\text{Se}$

**Year:** 2019

**Version:** Published version

**Copyright:** © 2019 American Physical Society

**Rights:** In Copyright

**Rights url:** <http://rightsstatements.org/page/InC/1.0/?language=en>

**Please cite the original version:**

Wisniewski, J., Urban, W., Czerwinski, M., Kurpeta, J., Plochocki, A., Pomorski, M., Rzaca-Urban, T., Sieja, K., Canete, L., Eronen, T., Geldhof, S., Jokinen, A., Kankainen, A., Moore, I. D., Nesterenko, D. A., Penttilä, H., Pohjalainen, I., Rinta-Antila, S., de Roubin, A., & Vilén, M. (2019). Excited states in  $^{87}\text{Br}$  populated in  $\beta$  decay of  $^{87}\text{Se}$ . *Physical Review C*, 100(5), Article 054331. <https://doi.org/10.1103/PhysRevC.100.054331>

## Excited states in $^{87}\text{Br}$ populated in $\beta$ decay of $^{87}\text{Se}$

J. Wiśniewski,<sup>1</sup> W. Urban,<sup>1</sup> M. Czerwiński,<sup>1</sup> J. Kurpeta,<sup>1</sup> A. Płochocki,<sup>1</sup> M. Pomorski,<sup>1</sup> T. Rząca-Urban,<sup>1</sup> K. Sieja,<sup>2</sup> L. Canete,<sup>3</sup> T. Eronen,<sup>3</sup> S. Geldhof,<sup>3</sup> A. Jokinen,<sup>3</sup> A. Kankainen,<sup>3</sup> I. D. Moore,<sup>3</sup> D. A. Nesterenko,<sup>3</sup> H. Penttilä,<sup>3</sup> I. Pohjalainen,<sup>3</sup> S. Rinta-Antila,<sup>3</sup> A. de Roubin,<sup>3</sup> and M. Vilén<sup>3</sup>

<sup>1</sup>*Faculty of Physics, University of Warsaw, ulica Pasteura 5, PL-02-093 Warsaw, Poland*

<sup>2</sup>*Université de Strasbourg, IPHC, CNRS, UMR7178, 67037 Strasbourg, France*

<sup>3</sup>*Department of Physics, University of Jyväskylä, P.O. Box 35, FIN-40014, Finland*



(Received 25 June 2019; revised manuscript received 23 September 2019; published 26 November 2019)

Excited levels in  $^{87}\text{Br}$ , populated in  $\beta$  decay of  $^{87}\text{Se}$ , have been studied by means of  $\gamma$ -ray spectroscopy using an array of broad energy Ge detectors.  $^{87}\text{Se}$  nuclei were produced by irradiating a natural Th target with 25-MeV protons. Fission products were extracted from the target chamber using the IGISOL technique, then separated on a dipole magnet and Penning trap (JYFLTRAP) setup. The scheme of excited levels of  $^{87}\text{Br}$  has been significantly extended. 114 new transitions and 51 new levels were established.  $\beta$  feedings and  $\log(ft)$  values of levels were determined. The upper limit for  $\beta$  feeding to the ground state of  $^{87}\text{Br}$  was determined to be 23(5)%. Ground state spin and parity  $5/2^-$  was confirmed, as suggested by previous studies. We also confirm the low-energy excited state at 6.02 keV. The ground state and two lowest excited states in  $^{87}\text{Br}$  were interpreted as the  $(\pi f_{5/2})^3_{j,j-1,j-2}$  triplet produced by the so-called anomalous coupling. The 333.61- and 699.26-keV levels were interpreted as  $\pi p_{3/2}$  and  $\pi p_{1/2}$  single-particle excitations. The  $9/2^+$  level reported previously as corresponding to the  $\pi g_{9/2}$  single-particle excitation is proposed to be an isomer with half-life 20 ns. Large-scale shell-model calculations performed in this work are in good agreement with experimental results.

DOI: [10.1103/PhysRevC.100.054331](https://doi.org/10.1103/PhysRevC.100.054331)

### I. INTRODUCTION

Evolution of nuclear collectivity in nuclei remains one of the most important aspects of nuclear structure studies. This work is a continuation of our previous studies in the “northeast” region of  $^{78}\text{Ni}$  [1–6]. Of particular interest is the understanding of how collectivity evolves above the  $N = 50$  closed shell. Another interesting aspect in this region is how the large excess of neutrons modifies the shell structure compared to the structure at the stability line. It has been predicted by various calculations that the excess of neutrons affects neutron density, resulting in quenching of shell effects [7]. Neutron-rich nuclei in the vicinity of doubly magic nuclei, such as  $^{78}\text{Ni}$ , provide a basis for testing such predictions. Excited states in nuclei from this region provide information on single-particle energies as well as on collectivity evolution just above the closed shell [8], providing input for testing nuclei with large excesses of neutrons [9]. Precise modeling of nuclear structure has direct impact on the  $r$ -process path occurring in type-II supernovae [10].

In our recent work on  $^{83}\text{As}$  [11] we discussed the single-particle energy of the  $\pi g_{9/2}$  orbital, which is crucial for describing medium-spin levels in the region. It is of high importance to confirm this result. This may be achieved by studying other nuclei in this region, such as  $^{87}\text{Br}$ . Medium-spin states of  $^{87}\text{Br}$  were recently studied in the neutron-induced fission of  $^{235}\text{U}$  [12]. Preliminary results suggest the presence of a  $9/2^+$  level corresponding to the  $\pi g_{9/2}$  orbital. To confirm this result, proper identification of spins and parities in  $^{87}\text{Br}$  is required, especially spin-parity of the ground state.

It was tentatively assigned to be  $5/2^-$  in a  $\beta$ -decay study of  $^{87}\text{Br}$  [13] to account for spins and parities in  $^{87}\text{Kr}$  populated in  $\beta$  decay of  $^{87}\text{Br}$ . To confirm this assignment and to determine spins and parities of excited states in  $^{87}\text{Br}$ , we have measured  $\gamma$  radiation following  $\beta$  decay of  $^{87}\text{Se}$ . The experiment was performed at the IGISOL facility [14] of the Accelerator Laboratory of the University of Jyväskylä, using an array of broad energy Ge (BEGe) detectors assembled there by the University of Warsaw group.

This work is organized as follows. After experimental details are given in Sec. II, results are described in Sec. III. This is followed by a discussion in Sec. IV, where results are interpreted in the shell-model framework and compared to large-scale shell-model calculations. The work is summarized in Sec. V.

### II. EXPERIMENTAL DETAILS

Neutron-rich  $^{87}\text{Se}$  were populated in fission induced by a 25-MeV, 9- $\mu\text{A}$  proton beam, irradiating a natural Th target. Fission products were separated using the IGISOL-4 setup [15]. Fission fragments were stopped in helium gas, then collimated and accelerated up to 30 keV using a sextupole ion guide (SPIG) electrode [16]. After separation using a  $55^\circ$  dipole magnet, the isobaric ion beam was electrostatically decelerated in a cooler-buncher [17] down to 100 eV, then sent in bunches to JYFLTRAP [14,18], a double Penning trap setup for isobaric purification and effective reduction of background. Only the purification trap was used. The

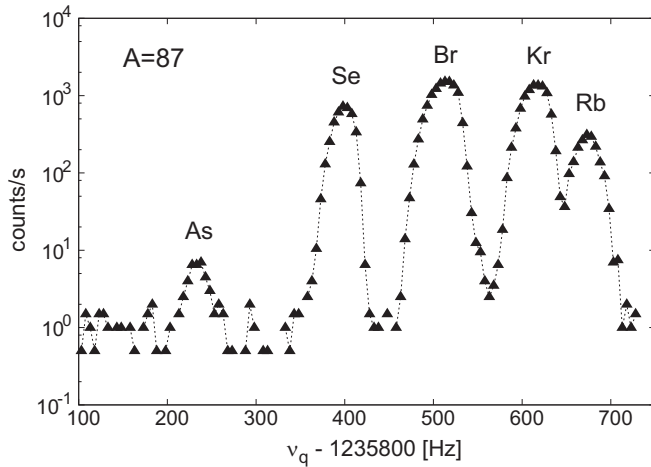


FIG. 1. Spectrum of singly charged ions with mass number  $A = 87$  obtained using a mass selective buffer-gas cooling technique [19] and detected on a MCP detector located behind the Penning traps. Peaks corresponding to various isotopes are marked with their element symbol.

separation technique is described in detail in Refs. [14,19]. In Fig. 1 we present the spectrum of ions with mass  $A = 87$  as function of quadrupolar excitation,  $\nu_q$ . The measurement was performed using a microchannel plate (MCP) located behind the Penning traps. As seen in Fig. 1, a monoisotopic beam of  $^{87}\text{Se}^+$  ions was delivered after the purification in the Penning trap. The rate on the MCP detector of  $^{87}\text{Se}^+$  was about 1000 ions/s. The duration of the purification-trap cycle was 101 ms.

Ions of  $^{87}\text{Se}^+$  were implanted into plastic tape in the focus point of the Ge array. During the measurement the tape was not moving. The detector setup is presented in Fig. 2. It consists of six high-resolution germanium detectors of 25% efficiency (BEGe) with thin carbon composite windows (0.6 mm) providing good transmission for low-energy  $\gamma$  rays. Those detectors (blue color in Fig. 2) were mounted in octagonal geometry around the implantation point in a plane perpendicular to the

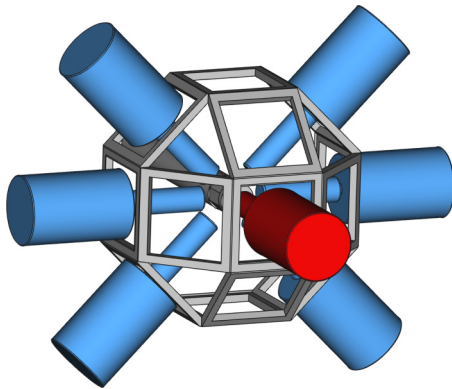


FIG. 2. Experimental setup used in this experiment.  $^{87}\text{Se}^+$  ions, released from JYFLTRAP, are implanted in the middle of a Ge array.  $\gamma$  rays emitted in  $\beta$  decay are registered by six BEGe detectors (blue) and one large-volume Ge detector (red). See text for more details.

ion beam direction. Resolution of BEGe detectors was 0.4 and 2.0 keV at 5.9 and 1332.5 keV, respectively. In addition one large Ge detector with efficiency 70% was installed to register high-energy  $\gamma$  rays. It was mounted in a position perpendicular with respect to the plane of other detectors (red color in Fig. 2). Vacuum chamber windows were made of thin Kapton foil (0.126 mm) to minimize absorption of low-energy  $\gamma$  rays. Each of the Kapton windows was facing one of the BEGe detectors. The window in front of the large detector was covered with thin metal foil.

Data were collected in triggerless mode using digital gamma finder cards (DGF). Collected data was ordered in time and sorted into various one- and two-dimensional histograms for further analysis.

### III. RESULTS

#### A. $\beta$ -decay scheme of $^{87}\text{Br}$

$\beta$  decay of  $^{87}\text{Se}$  was measured for the first time by Zendel *et al.* [20].  $^{87}\text{Se}$  nuclei were produced in thermal neutron induced fission of  $^{235}\text{U}$  then separated from other fission products using subsequent chemical separation. A partial scheme of excited states in  $^{87}\text{Br}$  was proposed. Based on intensity balances,  $\log(ft)$  values were calculated and tentative spins and parities for levels were proposed.

The partial scheme of excited states obtained in this work is presented in Fig. 3. It is based on  $\gamma\gamma$  coincidences sorted within a 500 ns window. Examples of gated spectra are shown in Figs. 4(a)–4(c), illustrating quality of the data. The new data extend the level scheme reported in Ref. [20] by 114 new transitions and 51 new levels.

For clarity, levels observed above 2919.49-keV level are not shown in Fig. 3. All transitions and levels observed in this work are listed in Table I. Note that energy values presented in Fig. 3 are transition energies, corrected for the recoil of the nucleus, while values reported in Table I are measured  $\gamma$ -ray energies.  $\gamma$ -ray intensities are obtained from  $\gamma$ -singles spectra.

No direct measurement of absolute intensities of transitions in  $^{87}\text{Br}$  was done in the present work. However, because during our measurement the tape was not moving, we could assume that  $\beta$  decay of  $^{87}\text{Se}$  to  $^{87}\text{Br}$  and later to  $^{87}\text{Kr}$  occurs under radioactive equilibrium. Therefore, we used the absolute intensity, 22.0(3), of the 1419.71-keV transition in  $^{87}\text{Kr}$  [21] to calculate absolute intensity (per 100  $\beta$  decays) of lines in  $^{87}\text{Br}$ . The results are shown in Table I as  $I_{\text{tot}}$ . Absolute intensity values include correction for the internal conversion effect, taken as a mean theoretical value for  $M1$  and  $E2$  multipolarity. Internal conversion coefficients were calculated for  $\gamma$  rays with energies below 300 keV using BRICC code [22].

We confirm the 242.55-, 334.0-, 468.0-, 573.2-, 710.5-, 1167.6-, 1305.0-, and 3744.5-keV transitions reported earlier. The 242.55-, 572.67-, and 710.16-keV transitions are feeding the level at 6.02 keV, newly observed in Ref. [12], instead of the ground state, as reported in [20]. The 1878.1- and 3683.8-keV transitions from [20] were not observed in this work; however, we report 1883.2- and 3688.8-keV transitions, feeding the ground state and the 248.56-keV level, respectively.

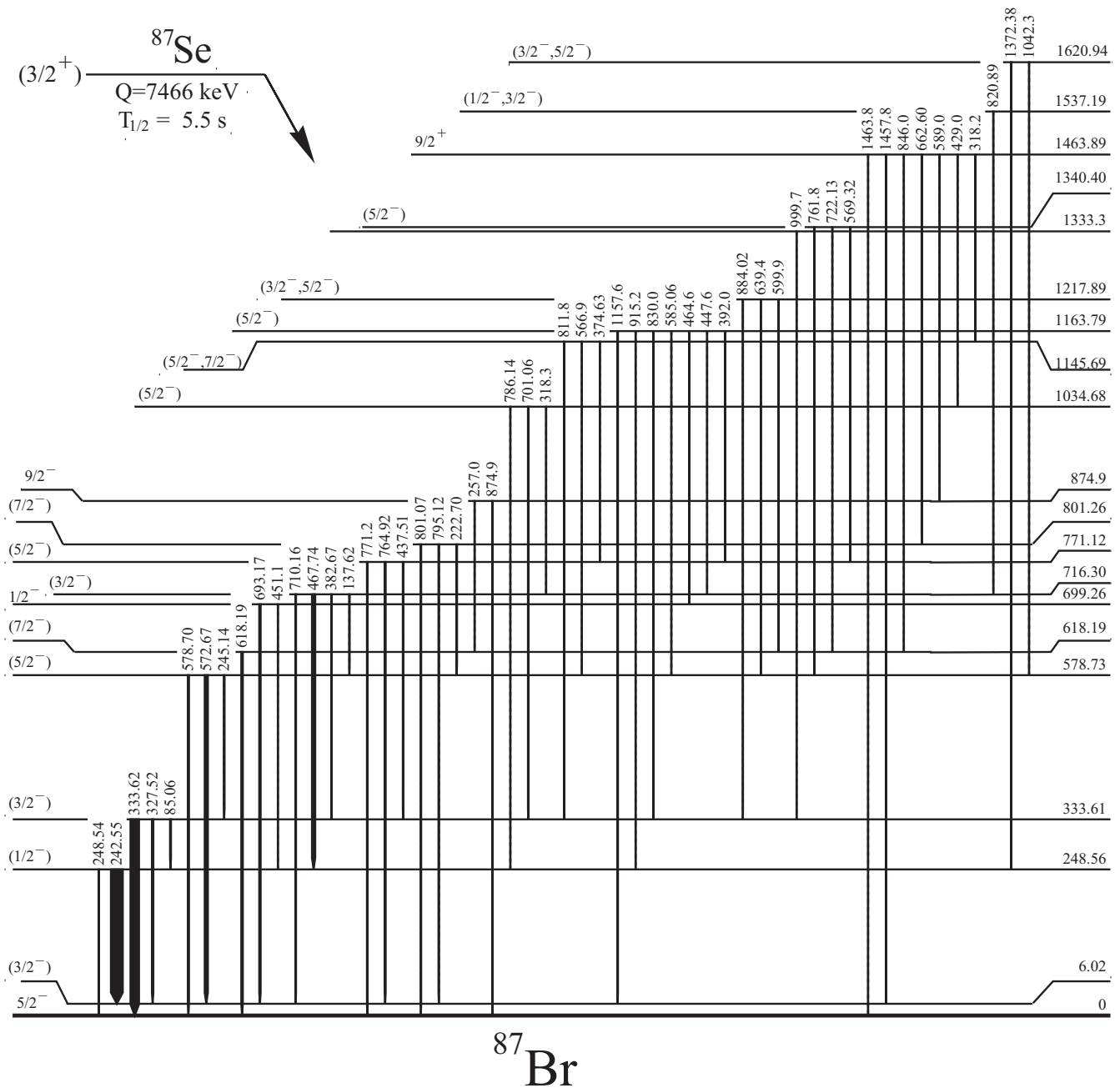


FIG. 3. Part I. Partial scheme of excited levels in  $^{87}\text{Br}$ , populated in  $\beta$  decay of  $^{87}\text{Se}$ , as observed in the present work. Thickness of arrows representing transitions is proportional to their relative  $\gamma$ -ray intensities.

The 3926-keV transition reported in Ref. [20] as feeding the ground state is not seen in our data.

We do observe the 1463.8-keV level, which was reported in prompt- $\gamma$  fission [12] and assigned spin-parity  $9/2^+$ . Such high spin is not expected to be populated directly in  $\beta$  decay of the  $(3/2^+)$  ground state of  $^{87}\text{Se}$  but this level may be populated by  $\gamma$  decays of levels with lower spins which are located above the  $9/2^+$  level. Indeed, we observe the 388.07- and 419.9-keV transitions from the 1851.9- and 1883.59-keV levels, respectively, feeding the  $9/2^+$  level.

### B. $\log(ft)$ and $\beta$ feeding

Based on intensity balances the  $\log(ft)$  values were calculated using Fermi function tables [23]. Because of low energy and high conversion coefficient we do not observe the decay of the 6.02-keV level to the ground state. Therefore, we were not able to calculate  $\beta$  feeding and corresponding  $\log(ft)$  values for this level. Absolute  $\gamma$ -ray intensities feeding the 6.02-keV level and ground state are equal to 47(4)% and 30(1)%, respectively.  $\beta$  feeding of the ground state was estimated in Ref. [20] to be 32%. Later, Lin *et al.* [24] reported a new

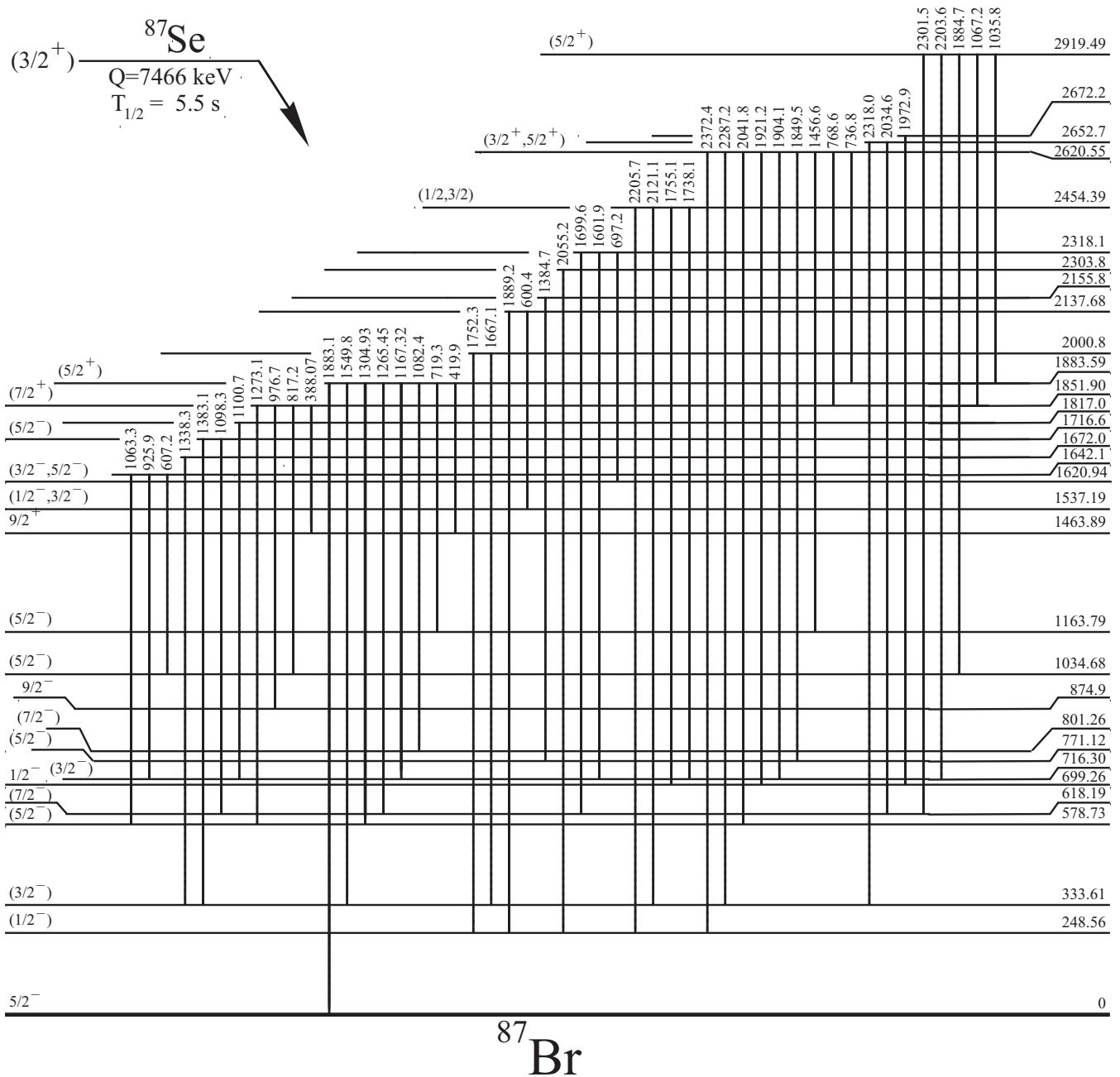


FIG. 3. Part II. (Continued.)

value of 42.5%. We can calculate an upper limit for this value, assuming that there is no  $\beta$  feeding to the 6.02-keV level, which decays to the ground state. Because summed, absolute intensity of transitions feeding the ground state is 77(5)% and the  $\beta$ - $n$  decay channel of  $^{87}\text{Se}$  accounts for 0.36% decays, we estimate the upper limit for the feeding of the ground state to be 23(5)%. The obtained value is lower than values reported earlier [20,24] and may be even lower if the 6.02-keV level receives any direct population in  $\beta$  decay of  $^{87}\text{Se}$ .

### C. Spin and parity assignments

Systematics of  $N = 53$  isotones suggest  $(3/2^+)$  spin-parity for the ground state of  $^{87}\text{Se}$ , the mother nucleus of  $^{87}\text{Br}$ . This value is supported by shell-model calculations and interpreted in terms of the so-called  $j - 1$  anomaly [2].

Of prime importance for spin-parity assignments of excited states in  $^{87}\text{Br}$  is the knowledge of its ground-state spin and parity. In the compilation [25] the  $3/2^-$  value was proposed, based on systematics and the observed  $\log(ft)$  values. Later,



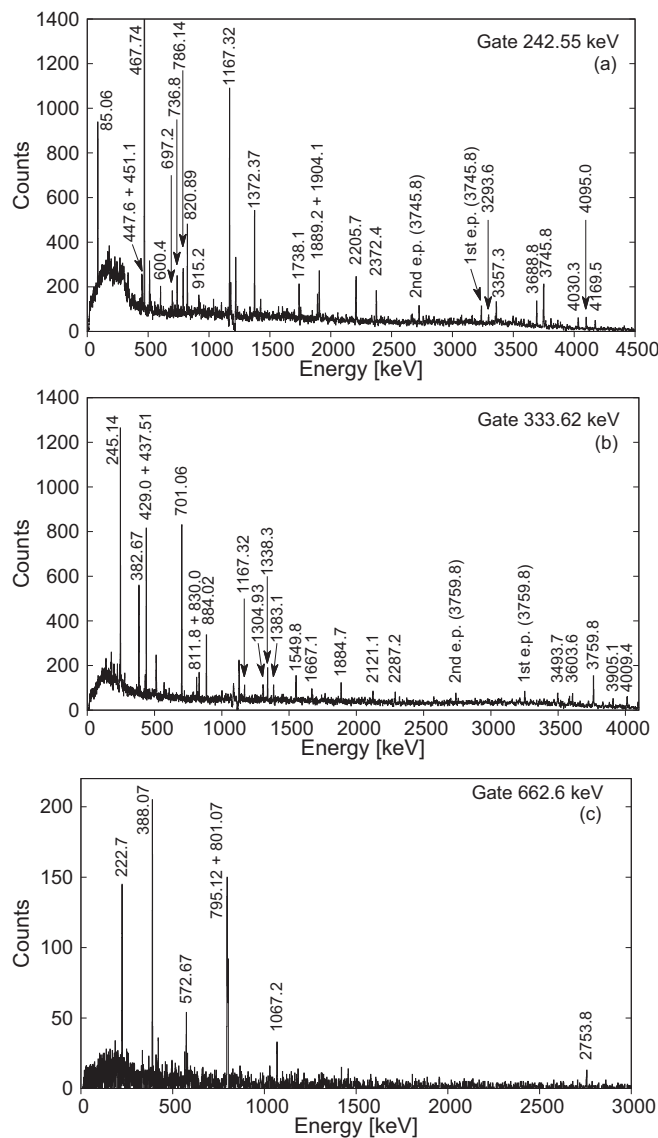


FIG. 4. Examples of gated  $\gamma$ -ray spectra obtained in this work. (a)  $\gamma$ -ray spectrum gated on the 242.55-keV transition. (b)  $\gamma$ -ray spectrum gated on the 333.62-keV transition. (c)  $\gamma$ -ray spectrum gated on the 662.60-keV transition. Energies are in keV.

this was changed to  $5/2^-$ , to account for measured spin values in  $^{87}\text{Kr}$ . [26]. Recent work [12] on low-to-medium spin states in  $^{87}\text{Br}$ , populated in neutron-induced fission of  $^{235}\text{U}$ , reported bandlike structures in this nucleus, supporting spin-parity  $5/2^-$  for the ground state of  $^{87}\text{Br}$ . The  $5/2^-$  value agrees with the  $\beta$ -feeding upper limit of 23(5)% and  $\log(ft) = 6.3$  for the  $^{87}\text{Br}$  ground state estimated in the present work and is consistent with the first forbidden  $\beta$  decay from the  $(3/2^+)$  g.s. state of  $^{87}\text{Se}$ . Therefore we adopt spin-parity  $5/2^-$  for the ground state of  $^{87}\text{Br}$ .

Calculated  $\log(ft)$  values alongside observed branchings were used in this work to propose spins and parities to excited levels in  $^{87}\text{Br}$ . We do not observe enhanced  $\beta$  decays to low-energy excited states in  $^{87}\text{Br}$ . The obtained  $\log(ft)$  values, varying in a range from 6 to 8, may be associated with first-

forbidden  $\beta$  transitions, suggesting negative parity for most of the low-spin excitations populated in  $\beta$  decay of the  $(3/2^+)$  ground state of  $^{87}\text{Se}$ . Negative parity for low-energy, low-spin excitations of  $^{87}\text{Br}$  was also proposed in Ref. [12].

The 874.9- and 618.19-keV levels were observed in the  $(^{235}\text{U} + n)$  fission measurement [12,27] and tentatively assigned spins  $9/2^-$  and  $7/2^-$ , respectively. Those levels are probably members of a collective structure built on top the ground state. We do not observe any feeding of the 874.9-keV level in  $\beta$  decay. This suggests that the spin of this level differs from the spin of the  $^{87}\text{Se}$  ground state by more than two units. Therefore, we support the  $9/2^-$  spin-parity for the 874.9-keV level. The 618.19-keV level decays only to the ground state, therefore spin higher than  $5/2^-$  is expected for this level. Its  $\log(ft) = 9.2$  calculated for the first-forbidden, unique  $\beta$  decay is consistent with the  $7/2^-$  spin assignment for this level.

Angular correlations for the 589.0–874.9-keV cascade reported in Refs. [12,27] suggest mixed  $Q + D$  character for the 589.0-keV transition and are consistent with  $(9/2^+)$  spin-parity for the 1463.89-keV level. We observe small  $\beta$  feeding 0.7(2)% to this state, which is unexpected considering the three units of angular momentum difference between the spin of the g.s. of the mother nucleus and the 1463.89-keV level. Because of the relatively large  $Q_\beta$  value there may be some amount of unobserved intensity feeding this state via a number of undetected weak  $\gamma$  transitions due to the so-called pandemonium effect [28]. Therefore, the observed  $\beta$ -feeding value should be treated as an upper limit rather than a firm value.

The 1463.89-keV level is fed by the 388.07-keV decay of the 1851.90-keV level, as seen in Fig. 4(c), showing  $\gamma$  spectrum gated on the 662.60-keV line, which depopulates the 1463.89-keV level. The observed decay pattern of the 1851.90-keV level suggest that its spin cannot be lower than  $7/2$ , because it has prompt decays to  $9/2^+$ , 1463.89-keV and  $9/2^-$ , 874.9-keV levels. We propose spin-parity  $7/2^+$  for this level.

The 1883.59-, 2620.55-, and 2919.49-keV levels receive relatively strong feeding in  $\beta$  decay resulting in  $\log(ft)$  lower than  $\log(ft)$  values of other levels with similar excitation energies. Considering also their decays to the  $9/2^+$ , 1463.89-keV level and to each other, we propose that these three levels are populated in allowed  $\beta$ -decay and have positive parity. The observed branchings from the three levels suggest spin-parities of  $(5/2^+)$ ,  $(3/2^+)$ ,  $5/2^+$ , and  $(5/2^+)$  for the 1883.59-, 2620.55-, and 2919.49-keV levels, respectively.

Based on the  $E2$  character of the 795.12-keV transition and the observed decay pattern of the 801.26-keV level, spin-parities of  $3/2^-$  and  $7/2^-$  were assigned to the 6.02- and 801.26-keV levels, respectively [12,27]. The  $7/2^-$  spin-parity for the 801.26-keV level is consistent with our  $\log(ft) = 9.0$ , calculated for the first-forbidden unique  $\beta$  transition. We also uphold the  $3/2^-$  assignment to the 6.02-keV level, reported in Refs. [12,27].

Strong  $\beta$  feeding is observed to the 248.56- and 333.61-keV levels. The  $\log(ft)$  values of 6.5(2) and 6.4(1), determined for these levels, respectively, suggests spin values of  $1/2$ ,  $3/2$ , and  $5/2$  for both levels. The 248.56-keV level

TABLE I. Energies of excited levels,  $E_{\text{lev}}$ , and spins  $I^\pi$ , with beta feedings and corresponding  $\log(ft)$  values, alongside observed gamma transitions depopulating given excited levels, described by energy of  $\gamma$  ray,  $E_\gamma$ , and transition intensities per 100 decays,  $I_{\text{tot}}$ . Values presented in bold were calculated for first-forbidden unique  $\beta$  transitions. See text for more information.

$E_{\text{lev}}$ (keV)	$I^\pi$	$\beta$ feed. (%)	$\log(ft)$	$E_\gamma$ (keV)	$I_{\text{tot}}$
0.0	$5/2^-$	$\leq 23(5)$	$\geq 6.3(2)$		
6.02(8)	$(3/2^-)$				
248.56(6)	$(1/2^-)$	11.1(3.1)	6.5(2)	242.55(2)	26.5(2.8)
				248.54(9)	0.28(5)
333.61(3)	$(3/2^-)$	12.8(1.8)	6.4(1)	85.06(5)	1.7(3)
				327.52(7)	3.2(4)
				333.62(4)	18.9(1.3)
578.73(4)	$(5/2^-)$	3.0(1.0)	7.0(3)	245.14(4)	1.8(2)
				572.67(5)	7.1(9)
				578.70(8)	2.6(2)
618.19(8)	$(7/2^-)$	1.9(4)	<b>9.2(2)</b>	618.19(8)	3.5(4)
699.26(8)	$1/2^-$	1.8(4)	7.2(2)	451.1(2)	0.16(2)
				693.17(4)	3.3(3)
716.30(6)	$(3/2^-)$	6.0(1.0)	6.6(2)	137.62(5)	1.2(2)
				382.67(5)	0.72(7)
				467.74(2)	7.2(8)
				710.16(8)	1.8(2)
771.12(5)	$(5/2^-)$	3.4(4)	6.9(1)	437.51(5)	1.1(1)
				764.92(9)	2.4(2)
				771.2(1)	1.4(1)
801.26(4)	$(7/2^-)$	2.6(5)	<b>9.0(2)</b>	222.70(5)	1.5(2)
				795.12(6)	1.5(3)
				801.07(8)	1.2(1)
874.9(2)	$9/2^-$	$-0.01(12)$		257.0(1)	0.05(2)
				874.8(2)	0.5(1)
1034.68(4)	$(5/2^-)$	0.6(2)	7.5(3)	318.3(3)	0.1(1)
				701.06(4)	1.4(1)
				786.14(8)	0.22(3)
1145.69(8)	$(5/2^-, 7/2^-)$	0.6(1)	7.5(1)	374.63(8)	0.23(5)
				566.9(2)	0.15(3)
				811.8(2)	0.18(3)
1163.79(5)	$(5/2^-)$	2.2(4)	6.9(1)	392.0(2)	0.15(5)
				447.6(1)	0.18(5)
				464.6(2)	0.05(1)
				585.06(8)	0.49(7)
				830.0(2)	0.22(3)
				915.2(2)	0.12(3)
				1157.6(2)	1.3(3)
1217.88(6)	$(3/2^-, 5/2^-)$	0.9(1)	7.3(1)	599.9(1)	0.09(2)
				639.4(1)	0.21(3)
				884.02(8)	0.62(6)
1333.3(2)		0.09(2)	8.3(2)	999.7(2)	0.09(2)
1340.40(7)	$(5/2^-)$	0.7(1)	7.4(1)	569.32(8)	0.39(7)
				722.13(8)	0.22(5)
				761.8(3)	0.11(2)
1463.89(7)	$9/2^+$	$<0.7(2)$		318.2(2)	0.1(1)
				429.0(2)	0.28(4)
				589.0(2)	0.30(6)
				662.60(8)	0.9(1)
				846.0(2)	0.10(3)
				1457.8(2)	0.43(9)
				1463.8(3)	0.1(1)
1537.19(8)	$(1/2^-, 3/2^-)$	0.2(1)	7.8(5)	820.89(7)	0.61(8)
1620.94(9)	$(3/2^-, 5/2^-)$	1.0(1)	7.1(1)	1042.3(3)	0.19(5)
				1372.37(7)	1.0(1)

TABLE I. *Continued.*

$E_{\text{lev}}$ (keV)	$I^\pi$	$\beta$ feed. (%)	$\log(ft)$	$E_\gamma$ (keV)	$I_{\text{tot}}$
1642.1(2)		0.6(1)	7.4(1)	607.2(4)	0.12(3)
				925.9(3)	0.09(2)
				1063.3(3)	0.39(6)
1672.0(2)		0.4(1)	7.5(1)	1338.3(2)	0.38(5)
1716.6(2)	(5/2 <sup>-</sup> )	0.4(1)	7.5(1)	1098.3(2)	0.13(3)
				1383.1(3)	0.26(4)
1817.0(2)		0.16(3)	7.9(2)	1100.7(2)	0.16(3)
1851.90(7)	(7/2 <sup>+</sup> )	<1.0(2)		388.07(7)	1.03(9)
				817.2(2)	0.10(3)
				976.7(2)	0.22(3)
				1273.1(2)	0.7(1)
1883.59(4)	(5/2 <sup>+</sup> )	7.3(8)	6.2(1)	419.9(2)	0.21(4)
				719.3(2)	0.18(5)
				1082.4(1)	0.7(1)
				1167.32(5)	2.2(3)
				1265.45(8)	0.35(9)
				1304.93(7)	2.4(2)
				1549.8(2)	0.41(6)
				1883.1(2)	1.8(3)
2000.8(2)		0.34(5)	7.5(1)	1667.1(3)	0.22(3)
				1752.3(3)	0.13(3)
2137.68(9)		0.5(1)	7.3(2)	600.4(1)	0.21(7)
				1889.2(1)	0.25(4)
2155.8(2)		0.17(5)	7.7(3)	1384.7(2)	0.17(5)
2303.8(4)		0.10(2)	7.9(2)	2055.2(4)	0.10(2)
2318.1(1)		0.3(1)	7.3(2)	697.2(1)	0.12(4)
				1601.9(4)	0.16(4)
				1699.6(5)	0.07(4)
2454.39(8)	(1/2,3/2)	1.6(2)	6.6(1)	1738.1(1)	0.42(5)
				1755.1(2)	0.30(4)
				2121.1(3)	0.22(4)
				2205.7(2)	0.67(9)
2620.55(5)	(3/2 <sup>+</sup> , 5/2 <sup>+</sup> )	3.0(3)	6.3(1)	736.8(1)	0.5(1)
				768.6(3)	0.10(3)
				1456.6(2)	0.18(5)
				1849.5(2)	0.29(7)
				1904.1(1)	0.76(9)
				1921.2(3)	0.13(3)
				2041.8(2)	0.48(5)
				2287.2(4)	0.24(4)
				2372.4(1)	0.40(6)
2652.7(2)		0.5(1)	7.1(2)	2034.6(2)	0.31(8)
				2318.0(6)	0.16(5)
2672.2(2)		0.3(1)	7.2(2)	1972.9(2)	0.33(6)
2919.49(9)	(5/2 <sup>+</sup> )	2.1(2)	6.3(1)	1035.8(2)	0.4(1)
				1067.2(2)	0.70(6)
				1884.7(2)	0.5(1)
				2203.6(2)	0.34(6)
				2301.5(2)	0.22(6)
3094.7(8)	(1/2,3/2)	0.10(3)	7.6(3)	2846.0(8)	0.10(3)
3542.3(5)	(1/2,3/2)	0.17(4)	7.1(2)	3293.6(5)	0.18(3)
3545.9(9)		0.17(2)	7.1(1)	3212.2(9)	0.18(3)
3606.0(3)	(1/2,3/2)	0.4(1)	6.7(2)	3357.3(3)	0.40(6)
3726(1)		0.14(4)	7.1(3)	3392(1)	0.14(4)
3748(1)	(3/2,5/2)	0.17(5)	7.0(3)	2977(1)	0.17(5)
3809.7(6)	(1/2,3/2)	0.14(4)	7.1(3)	3561.0(6)	0.14(4)
3825.6(5)	(1/2,3/2)	0.16(5)	7.0(3)	3126.2(5)	0.16(5)



TABLE I. *Continued.*

$E_{\text{lev}}$ (keV)	$I^\pi$	$\beta$ feed. (%)	$\log(ft)$	$E_\gamma$ (keV)	$I_{\text{tot}}$
3827.4(4)		0.4(1)	6.6(2)	3493.7(4)	0.40(7)
3902.8(3)	(1/2,3/2)	0.4(1)	6.6(2)	3203.4(3)	0.36(9)
3937.4(2)		0.8(1)	6.3(1)	3603.6(4)	0.36(7)
				3688.8(3)	0.41(6)
3994.4(2)	(1/2,3/2)	1.2(1)	6.1(1)	3294.9(3)	0.22(5)
				3745.8(2)	0.95(9)
4055.0(5)		0.3(1)	6.6(1)	3722.4(9)	0.17(4)
				3805.9(6)	0.17(3)
4093.5(2)		0.9(2)	6.1(2)	3759.8(2)	0.9(1)
4111.1(4)	(1/2,3/2)	0.13(5)	7.0(3)	3862.4(4)	0.13(5)
4210.5(7)		0.15(4)	6.8(2)	3876.8(7)	0.15(4)
4238.8(4)		0.30(5)	6.5(2)	3905.1(4)	0.30(5)
4279.0(4)	(1/2,3/2)	0.22(4)	6.6(2)	4030.3(4)	0.22(4)
4342.7(3)		0.7(1)	6.1(1)	2804.7(6)	0.19(3)
				4009.4(4)	0.52(7)
4343.7(4)	(1/2,3/2)	0.19(4)	6.7(2)	4095.0(4)	0.19(4)
4418.2(5)	(1/2,3/2)	0.21(4)	6.6(2)	4169.5(5)	0.21(4)
4424.1(6)		0.15(4)	6.7(2)	4090.4(6)	0.15(4)
4496.1(5)	(3/2,5/2)	0.21(5)	6.5(2)	3917.3(5)	0.21(5)
4605.7(3)	(5/2)	0.3(1)	6.3(2)	2753.8(3)	0.31(7)
4607.4(4)	(3/2,5/2)	0.4(1)	6.2(2)	4028.6(4)	0.36(7)
5383(2)		0.09(4)	6.2(4)	5049(2)	0.09(4)

decays predominantly to the  $3/2^-$ , 6.02-keV level and only weakly to the  $5/2^-$  ground state. Therefore we propose spin-parity  $1/2^-$  for this level. The dominating 333.62-keV decay of the 333.61-keV level to the  $5/2^-$  ground state suggest its  $M1 + E2$  multipolarity. Considering that the 333.61-keV level also decays by low-energy, 85.06-keV transition to the  $1/2^-$ , 248.56-keV level, we propose spin-parity  $3/2^-$  for the 333.61-keV level.

With spin-parity  $1/2^-$  for the 248.56-keV level, spin and parity of the 1034.68-keV level is not higher than  $5/2^-$ . This means that the multipolarity of the 429.0-keV decay from the 1463.89-keV level is  $M2$ , which may be surprising but as discussed below is possible.

The 578.73-keV level decays to the 6.02-keV level and the ground state. This, along with its  $\log(ft) = 7.0$ , suggest spin-parity of  $3/2^-$  or  $5/2^-$  for this level. We do not observe any decay to the  $1/2^-$ , 248.56-keV level. Therefore the  $3/2^-$  value is less likely. Another argument in favor of spin-parity  $5/2^-$  is the mixed  $D + Q$  multipolarity of the 222.70-keV decay from the 801.26-keV level [27].

The 699.26-keV level was not observed in the fission measurement [12,27]. This suggests its non-yrast character, and the dominating decay to the  $1/2^-$ , 6.02-keV level suggests spin value lower than  $3/2^-$ . We tentatively assign to this level spin-parity  $(1/2^-)$ , which is consistent with its decay pattern and its  $\log(ft) = 7.2$ .

Prompt, low-energy decays of the 716.30-keV level to both  $1/2^-$  and  $5/2^-$  levels strongly suggests spin-parity  $3/2^-$  for the 716.30-keV level.

Spin-parity assignments to other levels, consistent with our  $\log(ft)$  values and observed decay patterns, are listed in Table I and shown in Fig. 3.

#### D. Possible isomeric nature of the 1463.8-keV level

As pointed out above, the 429.0-keV transition from the 1463.89-keV level may have an  $M2$  multipolarity. At this transition energy one would expect the partial half-life for such decay to be at least 200 ns for an  $M2$  of 0.3 W.u. Considering the observed branching of the 429.0-keV transition from the 1463.89-keV level, this translates to a half-life of about 20 ns for the 1463.89-keV level. We also notice that according to spin-parity assignments the 1457.8-keV decay from the 1463.89-keV level should be an  $E3$  transition. An expected partial half-life for an  $E3$  transition of 3 W.u. at this energy is about 100 ns. This, again, translates to 20 ns half-life of the 1463.89-keV level when taking into account the observed branching for the 1457.8-keV decay. It is then likely that the 1463.89-keV level is an isomer with a half-life of about 20 ns. In the present work we were not able to observe half-lives that short because of the 25 MHz clock of the digital electronics and unfavorable timing of BEGe detectors. One may note that, with the above estimate being valid, the 1463.8-keV  $M2$  branch would correspond to about  $2 \times 10^{-4}$  W.u. only, which is much different from the assumed rate of 0.3 W.u. for the 429.0-keV branch. This would mean different structures of the 1034.68-keV level and the ground state.

## IV. DISCUSSION

### A. Proposed interpretation of levels

Single-particle (s.p.) configurations of low-energy excited states in odd-even  $N = 52$  isotones are due to proton orbitals located above the  $Z = 28$  closed shell, namely the  $\pi f_{5/2}$ ,  $\pi p_{3/2}$ , and  $\pi p_{1/2}$  negative-parity orbitals and the  $\pi g_{9/2}$

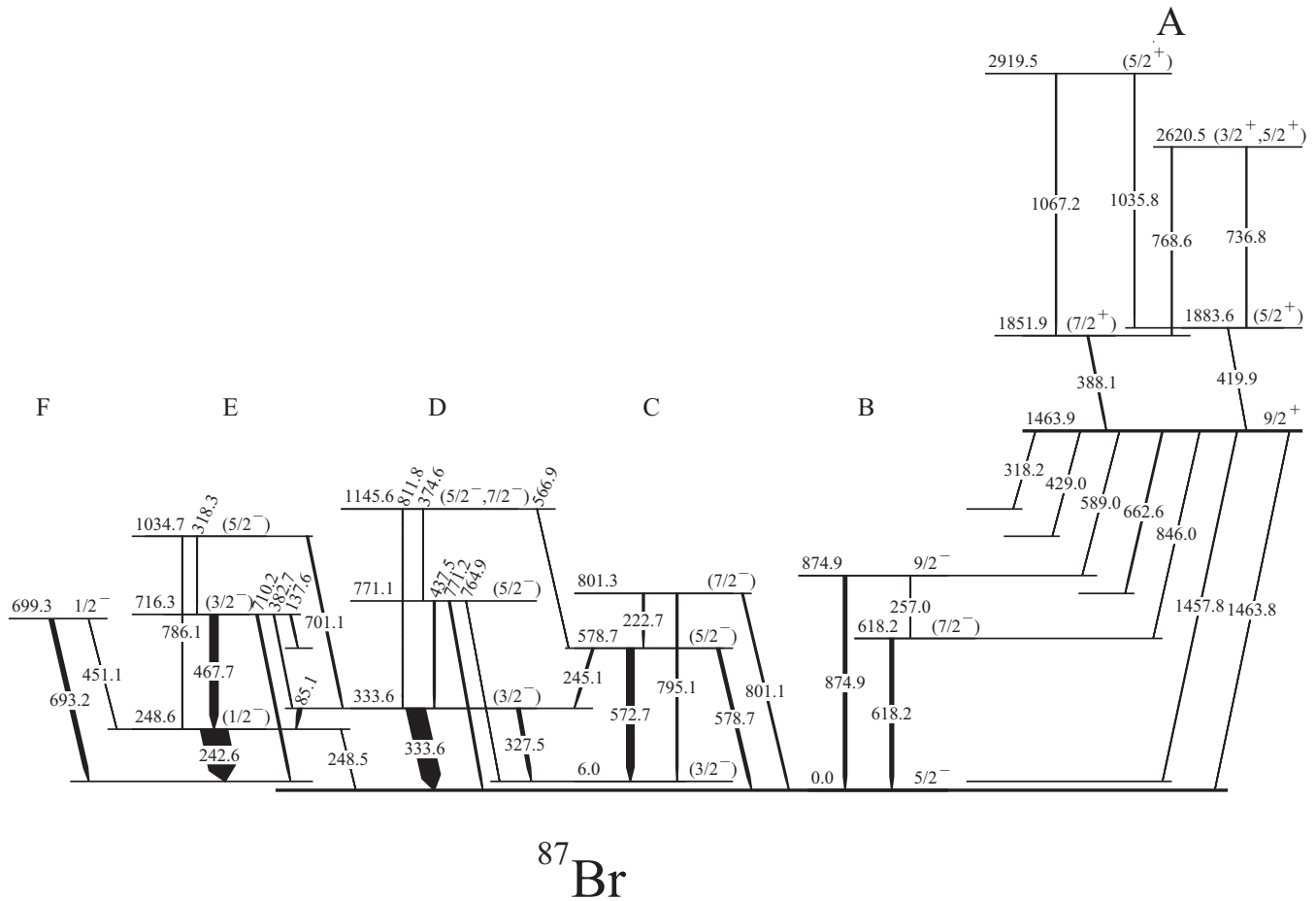


FIG. 5. Partial excitation scheme of  $^{87}\text{Br}$ , drawn from Fig. 3 to assist the discussion.

intruder orbital. One also expects quadrupole collective excitations built on those s.p. configurations. These excitations are expected to be due to vibrations in the even-even cores in this region, as discussed in our previous studies [1,2,6,29]. Furthermore, this collectivity coupled to a s.p. orbital with spin  $j$ , occupied by a few nucleons, may result in the so-called anomalous coupling, producing a multiplet of closely lying states with spins  $j, j-1, j-2$  [30], as observed in  $N=53$  even-odd isotones in this region [2–5]. Such states, also called “dressed” [31,32] can be interpreted as seniority coupling [33] or, more generally though less specific, as being due to the so-called Jahn-Teller effect [34], which removes the degeneracy of an orbital populated by several particles due to coupling to a collective excitation. In odd-even  $N=52$  isotones from the discussed region above  $Z=28$ , these particles can be found in the nearly degenerate  $\pi f_{5/2}$  and  $\pi p_{3/2}$  proton orbitals.

The mentioned effects will produce several low-energy excitations, where those with the same spin and parity will mix, because of similar origin and excitation energy. Therefore, one should not expect clear distinctions between various possible structures. In Fig. 5 we redraw low-energy excitations in  $^{87}\text{Br}$  shown in Fig. 3, unfolding the scheme into six different structures, labeled A to F, which are discussed below.

The ground state of  $^{87}\text{Br}$  with spin-parity  $5/2^-$  can be associated with the odd proton in the  $\pi f_{5/2}$  orbital. The ground state level is probably a collective structure, because according to the spherical shell-model scheme the  $\pi f_{5/2}$  orbital in  $^{87}\text{Br}$  is occupied by three protons. Therefore, one expects a triplet comprising three levels with spin  $5/2^-$  (the ground state),  $3/2^-$ , and  $1/2^-$ , produced by “anomalous coupling.” On top of the  $5/2^-$  ground state a collective structure is built, corresponding to vibrations of the  $^{86}\text{Se}$  core. The vibrational band, labeled B, comprises the 618.19- and 874.9-keV levels seen in this work and continues to higher spins, as reported in Ref. [27].

The  $3/2_1^-$ , first excited state at 6.02 keV is a candidate for the  $j-1$  member of the mentioned triplet. As shown in Fig. 6(a) the systematics of  $3/2_1^-$  excitations, drawn relative to the  $5/2_1^-$  levels, displays a trend characteristic for the  $j-1$  coupling, analogous to that observed in  $N=53$  isotones where three neutrons occupy the  $d_{5/2}$  orbital [2]. One can observe that the energy of the  $3/2_1^-$  level decreases with growing collectivity in  $N=52$  isotones, reaching a minimum for  $^{91}\text{Y}$ , between Sr and Zr, where quadrupole collectivity is known to be strong.

Because the  $3/2_1^-$  level has the same structure as the  $5/2^-$  ground state, one expects that there should be a vibrational

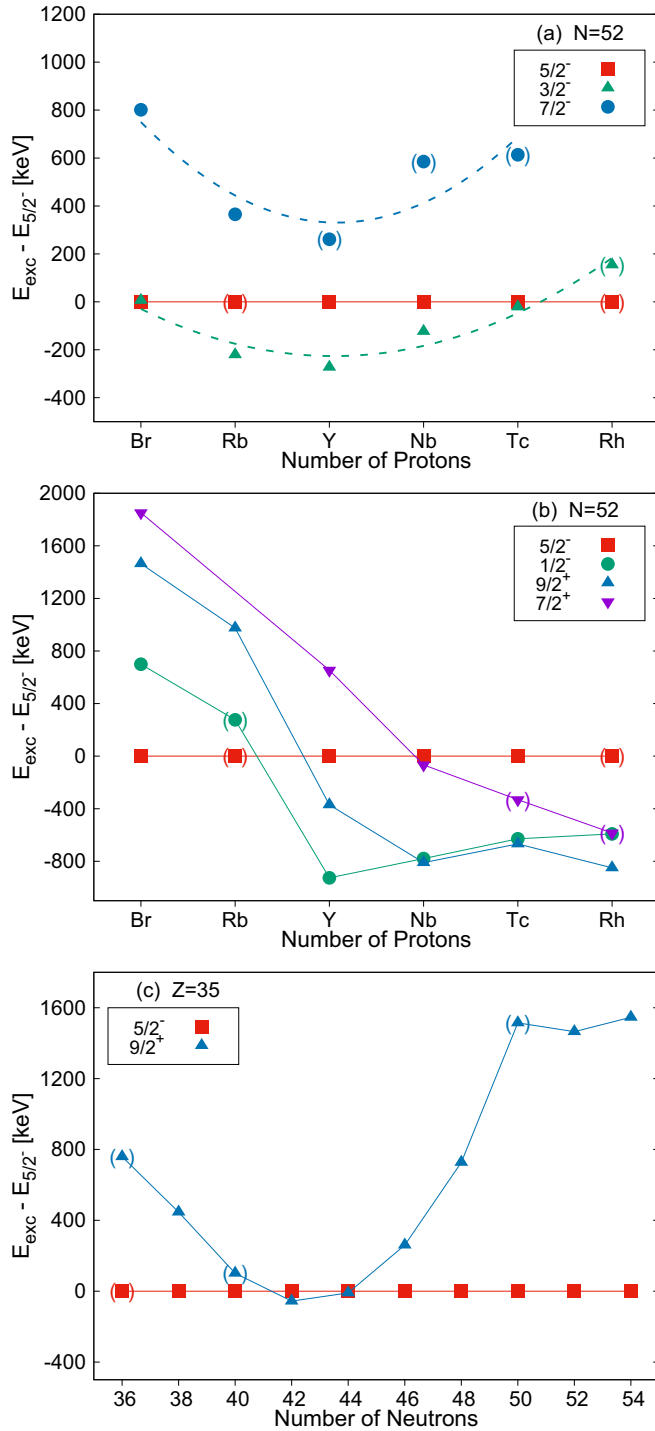


FIG. 6. Systematics of excited levels relative to  $5/2^-$  levels in  $N = 52$  [(a) and (b)] isotones and  $Z = 35$  isotopes (c). Data are taken from [35]. Lines are drawn to guide the eye.

cascade on top of the 6.02-keV level, analogous to that built on top of the ground state. The 578.73- and 801.26-keV levels are candidates for  $5/2^-$  and  $7/2^-$  excitations in this cascade, respectively. In Fig. 6(a) we show the energy trend for  $7/2^-$  levels decaying to the  $3/2_1^-$  levels in the  $N = 52$ , odd- $Z$  isotones in the region. Their excitations energies of

about 0.8 MeV follow the trend of  $3/2_1^-$  levels, which supports the proposed interpretation for the cascade C.

The 248.56-keV level can be interpreted as the  $j - 2$  anomalous coupling of the  $\pi(f_{5/2})^3$  g.s. multiplet. Cascade E comprises levels which most likely are collective excitations built on top of this level.

The 333.61-keV level, which has tentative spin-parity  $3/2^-$ , is a candidate for the  $\pi p_{3/2}$  s.p. excitation. Cascade D, built on top of this level, is strongly mixed with cascades C and E. Therefore, it is expected to be a complex mixture of  $\pi p_{3/2}$  and  $\pi(f_{5/2})^3$  configurations, rather than a single-particle  $\pi p_{3/2}$  state. This is also suggested by decays of numerous levels to both the 248.56- and 333.61-keV levels.

The 699.26-keV level with spin  $1/2^-$  (with label F) is a candidate for the  $\pi p_{1/2}$  s.p. excitation. The systematics of analogous states is shown in Fig. 6(b). The  $1/2^-$  excitation follows the trend of  $9/2^+$  levels, which are due to the  $\pi g_{9/2}$  s.p. excitation. In the shell-model scheme of s.p. levels, the  $\pi p_{1/2}$  orbital is close to the  $\pi g_{9/2}$  orbital. Therefore the systematics shown in Fig. 6(b) offers some support to the proposition that the 699.26-keV level corresponds to the  $\pi p_{1/2}$  s.p. excitation. However, one should remember that there may be another close-lying  $1/2^-$  level, which is due to the discussed  $j - 2$  anomalous coupling in the  $\pi(f_{5/2})^3$  configuration. More information is needed to identify the structure of the lowest two  $1/2^-$  levels in odd- $Z$ ,  $N = 52$  isotones in this region.

Finally, we discuss the structure labeled A in Fig. 5. The 1463.89-keV level has spin and parity  $9/2^+$ . Its numerous decays suggest that this level is a head of structure A (decays from other positive-parity levels to negative-parity levels are not shown here to simplify the picture). The configuration of the 1463.89-keV level can be seen as an odd proton in the  $\pi g_{9/2}$  orbital coupled to the  $^{86}\text{Br}$  core. The systematics shown in Fig. 6(b) supports this picture: with growing proton number excitation energy of the  $9/2_1^+$  level in odd- $Z$ ,  $N = 52$  isotones decreases quickly and drops below the  $1/2_1^-$  level. This behavior is connected with protons filling first the  $\pi p_{1/2}$  and then the  $\pi g_{9/2}$  orbital. The  $9/2^+$  level is located about 1 MeV above the  $1/2^-$  level from  $^{87}\text{Br}$  to  $^{91}\text{Y}$ . In  $^{93}\text{Nb}$  the ground state spin changes from  $1/2^-$  to  $9/2^+$ , which may be interpreted as filling completely the  $\pi p_{1/2}$  orbital and populating the  $\pi g_{9/2}$  orbital. The proposed nature of the  $9/2_1^+$  level in  $^{87}\text{Br}$  is further supported by the systematics of  $9/2_1^+$  levels in the  $Z = 35$  isotopes, shown in Fig. 6(c). In the neutron range  $36 < N < 50$  the energy of this excitation shows a deep minimum due to the interaction of the  $\pi g_{9/2}$  proton with neutrons filling the  $\nu g_{9/2}$  orbital. Above  $N = 50$  this interaction is not present, resulting in approximately constant energy of the  $9/2_1^+$  level.

## B. Shell-model calculations

To learn more about the nature of excited levels in  $^{87}\text{Br}$  we performed SM calculations. A model space comprising  $f_{5/2}$ ,  $p_{3/2}$ ,  $p_{1/2}$ ,  $g_{9/2}$  proton and  $d_{5/2}$ ,  $s_{1/2}$ ,  $g_{7/2}$ ,  $d_{3/2}$ ,  $h_{11/2}$  neutron orbitals outside  $^{78}\text{Ni}$  was used. The effective interaction was introduced in Refs. [33,36], but later its proton-proton part was updated to better reproduce experimental data at  $N = 50$ ,

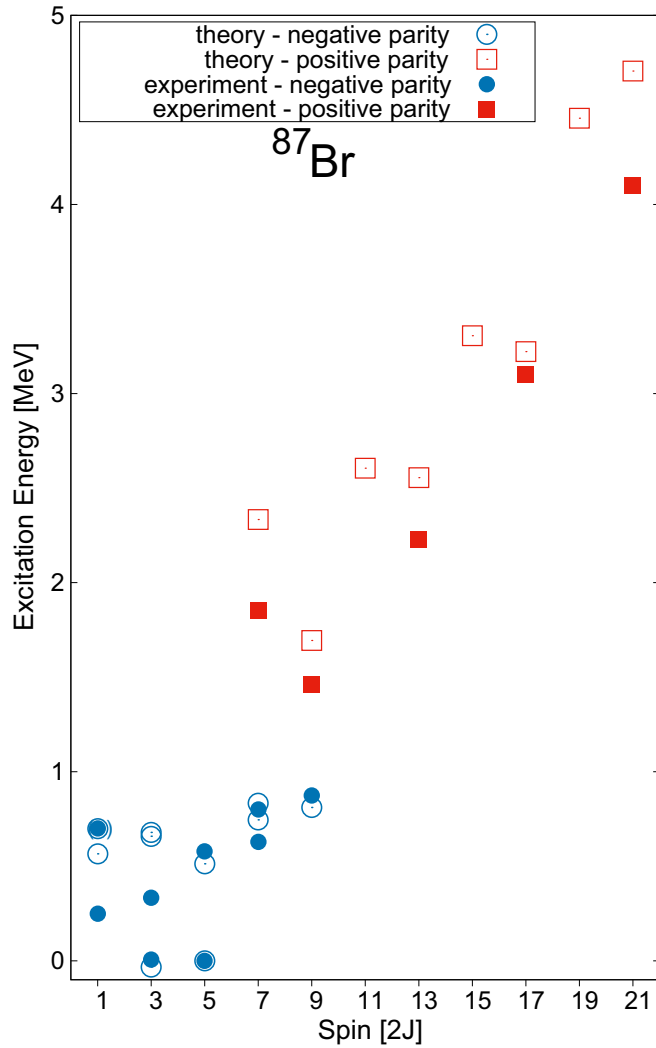


FIG. 7. Comparison of excited states populated in  $\beta$  decay of  $^{87}\text{Se}$  with shell-model calculations. Data are normalized to the  $5/2^-$  ground state. Experimental points presented above 2 MeV are taken from Ref. [12].

as described in [11]. Calculations were performed with the coupled-scheme code NATHAN [37]. Full diagonalizations in the model space were achieved. Similar calculations were performed in our previous works on  $N = 52$  and  $N = 53$  isotones [2–5,38].

Results of calculations are compared with experimental data in Fig. 7, where we also included energies of excitations built on the  $9/2^+$  level taken from Ref. [12]. The shell model predicts the  $3/2^-$  level to be the ground state with the  $5/2^-$  level 30 keV above: the results in the figure were normalized to the experimental  $5/2^-$  level. The overall scale of the observed excitations is fairly reproduced, describing well the  $9/2^+$  level seen at 1463.8 keV and the cascade on top of this level including the  $7/2^+$  member, identified in the present work. It would be interesting to identify experimentally other, nonfavored members of this cascade. Negative-parity excited states of  $^{87}\text{Br}$  are reproduced with accuracy 50 keV, except

TABLE II. Occupation of proton and neutron of excited states in  $^{87}\text{Br}$  calculated using the shell model.

$I^\pi$	Neutrons					Protons			
	$d_{5/2}$	$s_{1/2}$	$g_{7/2}$	$d_{3/2}$	$h_{11/2}$	$f_{5/2}$	$p_{3/2}$	$p_{1/2}$	$g_{9/2}$
$1/2^-$	1.72	0.09	0.05	0.08	0.06	4.11	1.98	0.68	0.23
$1/2_2^-$	1.64	0.17	0.05	0.08	0.06	3.61	2.48	0.72	0.19
$3/2^-$	1.60	0.15	0.07	0.10	0.08	3.90	2.57	0.30	0.23
$3/2_2^-$	1.62	0.18	0.05	0.09	0.06	3.62	2.66	0.51	0.21
$3/2_3^-$	1.63	0.13	0.06	0.11	0.07	4.71	1.74	0.33	0.22
$5/2^-$	1.61	0.13	0.07	0.12	0.08	4.48	1.97	0.33	0.23
$5/2_2^-$	1.54	0.27	0.05	0.09	0.05	3.58	2.80	0.43	0.18
$7/2^-$	1.59	0.21	0.04	0.11	0.05	4.52	1.96	0.33	0.19
$7/2_2^-$	1.63	0.20	0.04	0.09	0.04	3.92	2.53	0.35	0.20
$9/2^-$	1.73	0.11	0.03	0.09	0.04	4.57	1.90	0.31	0.22
$7/2^+$	1.56	0.13	0.06	0.11	0.14	3.97	1.68	0.30	1.05
$9/2^+$	1.57	0.14	0.08	0.14	0.07	4.03	1.57	0.28	1.12
$11/2^+$	1.73	0.08	0.03	0.10	0.06	4.08	1.53	0.30	1.09
$13/2^+$	1.56	0.22	0.04	0.13	0.04	3.90	1.68	0.31	1.11
$15/2^+$	1.75	0.09	0.02	0.04	0.10	4.37	1.36	0.22	1.05
$17/2^+$	1.78	0.05	0.02	0.09	0.07	4.30	1.41	0.22	1.08
$19/2^+$	1.22	0.03	0.03	0.05	0.67	4.66	1.59	0.24	0.51
$21/2^+$	1.76	0.06	0.03	0.12	0.03	3.82	1.83	0.29	1.07

the 248.56- and 333.61-keV levels, which are calculated about 250 keV higher than experimental values.

In Table II we present occupation numbers of proton and neutron orbitals for excited states of  $^{87}\text{Br}$  as obtained from SM calculations. As already mentioned, low-energy excitations in  $^{87}\text{Br}$  are produced by odd protons occupying different orbitals. Generally, the shell model predicts strong mixing of protons in  $p_{3/2}$  and  $f_{5/2}$  orbitals due to the small splitting between them (660 keV in  $^{79}\text{Cu}$ ) which is overcome by nondiagonal terms of the pairing interaction. The majority of calculated negative parity levels can be divided into two groups of states that are connected by the strongest  $B(E2)$  transitions: the first group, with a slight dominance of one proton-hole component  $f_{5/2}^{-1}$ , includes the first calculated level of each spin between  $5/2^-$  and  $13/2^-$ . The second group, based on the  $p_{3/2}^3$  configuration, contains  $3/2_1^-$  and the second calculated states  $5/2_2^-$ ,  $7/2_2^-$ ,  $9/2_2^-$ . However, the  $5/2_2^-$  state has a strong admixture of the  $f_{5/2}^3$  configuration as does the second  $3/2^-$ . The third calculated  $3/2^-$  state, nearly degenerate with the second one, exhibits a more single-particle nature ( $f_{5/2}^6 p_{3/2}^1$  configuration). As can be seen from the table, both calculated  $1/2^-$  states contain  $\approx 0.7$  particle in the  $\pi p_{1/2}$  orbital. Its occupation is also significant in the  $3/2_2^-$  state. The too high energy of the  $1/2_1^-$  and  $3/2_2^-$  levels may thus indicate that the position of the  $\pi p_{1/2}$  orbital in this region can be lower than assumed in the shell-model interaction, i.e.,  $\approx 2$  MeV above the  $\pi f_{5/2}$  level in  $^{79}\text{Cu}$ . Note that the only available spectroscopic study of  $^{79}\text{Cu}$  [39] did not provide any spin-parity assignments, and the Monte-Carlo shell-model calculations presented in the same work predict a  $1/2^-$  level with a strong single-particle component also at 2 MeV. A systematic study of low-energy levels in odd-proton nuclei can thus provide

the missing information about the actual position of the  $\pi p_{1/2}$  shell in the nickel core.

The structure of calculated positive parity levels is less complex. Except for the  $19/2^+$  state predicted to involve the neutron excitation to the  $h_{11/2}$  orbital, all the remaining states are excitations of one proton to the  $\pi g_{9/2}$ . The energy of the  $9/2^+$  state is fairly well reproduced and its calculated wave function confirms the presence of the  $\pi g_{9/2}$  orbital at 1463.89-keV level.

## V. SUMMARY

We have observed excited states in  $^{87}\text{Br}$  populated in  $\beta$  decay of  $^{87}\text{Se}$ . The level scheme of excited states was significantly extended with 114 new transitions and 51 new levels. Ground state  $\beta$  feeding of 23(5)% was determined. We support the spin-parity  $5/2^-$  of the ground state, suggested in previous studies [12,26]. We also confirm the low-energy excited state at 6.02 keV, reported in Refs. [12,27], which was not observed before in  $\beta$ -decay measurements.

The  $9/2^+$  level at 1463.89-keV is confirmed to be the  $\pi g_{9/2}$  single-particle excitations. The observed decays from

this level suggest that it may be an isomer with a half-life of about 20 ns. Experimental data fits well the systematics of  $N = 52$  isotones, which suggest that collectivity increases with the growing proton number, and reaches its maximum in the mid shell at  $^{91}\text{Y}$ .

Large-scale shell-model calculations performed in this work reproduce well the experimental scheme, including medium-spin excitations reported in Refs. [12,27]. Good agreement with experimental data supports the interpretation proposed in this work: there is a clear indication of the presence of the  $\pi g_{9/2}$  s.p. level at 1.5 MeV. In addition to s.p. excitations involving  $\pi f_{5/2}^5$ ,  $\pi p_{3/2}^1$ , and  $\pi p_{1/2}^1$  structures, the shell model predicts a number of excitations with moderate collectivity, which also fit well the experimental scheme.

## ACKNOWLEDGMENTS

This work has been supported by the National Science Centre under Contracts No. DEC-2013/09/B/ST2/03485 and No. DEC-2018/29/N/ST2/00707 and by the Academy of Finland under the Finnish Centre of Excellence Programme 2012-2017 (Project No. 251353, Nuclear and Accelerator-Based Physics Research at JYFL).

- 
- [1] M. Czerwiński, T. Rząca-Urban, K. Sieja, H. Sliwinska, W. Urban, A. G. Smith, J. F. Smith, G. S. Simpson, I. Ahmad, J. P. Greene, and T. Materna, *Phys. Rev. C* **88**, 044314 (2013).
  - [2] T. Rząca-Urban, M. Czerwiński, W. Urban, A. G. Smith, I. Ahmad, F. Nowacki, and K. Sieja, *Phys. Rev. C* **88**, 034302 (2013).
  - [3] M. Czerwiński, T. Rząca-Urban, W. Urban, P. Bączyk, K. Sieja, B. M. Nyakó, J. Timár, I. Kuti, T. G. Tornyi, L. Atanasova, A. Blanc, M. Jentschel, P. Mutti, U. Köster, T. Soldner, G. de France, G. S. Simpson, and C. A. Ur, *Phys. Rev. C* **92**, 014328 (2015).
  - [4] M. Czerwiński, T. Rząca-Urban, W. Urban, P. Bączyk, K. Sieja, J. Timar, B. M. Nyakó, I. Kuti, T. G. Tornyi, L. Atanasova, A. Blanc, M. Jentschel, P. Mutti, U. Köster, T. Soldner, G. de France, G. S. Simpson, and C. A. Ur, *Phys. Rev. C* **93**, 034318 (2016).
  - [5] M. Czerwiński, K. Sieja, T. Rząca-Urban, W. Urban, A. Plochocki, J. Kurpeta, J. Wiśniewski, H. Penttilä, A. Jokinen, S. Rinta-Antila, L. Canete, T. Eronen, J. Hakala, A. Kankainen, V. S. Kolhinen, J. Koponen, I. D. Moore, I. Pohjalainen, J. Reinikainen, V. Simutkin, A. Voss, I. Murray, and C. Nobs, *Phys. Rev. C* **95**, 024321 (2017).
  - [6] T. Materna, W. Urban, K. Sieja, U. Köster, H. Faust, M. Czerwiński, T. Rząca-Urban, C. Bernards, C. Fransen, J. Jolie, J.-M. Regis, T. Thomas, and N. Warr, *Phys. Rev. C* **92**, 034305 (2015).
  - [7] J. Dobaczewski, I. Hamamoto, W. Nazarewicz, and J. A. Sheikh, *Phys. Rev. Lett.* **72**, 981 (1994).
  - [8] M. G. Porquet, A. Astier, D. Verney, Ts. Venkova, I. Deloncle, F. Azaiez, A. Buta, D. Curien, O. Dorvaux, G. Duchêne, B. J. P. Gall, F. Khalfallah, I. Piqueras, M. Rousseau, M. Meyer, N. Redon, O. Stézowski, and A. Bogachev, *Phys. Rev. C* **84**, 054305 (2011).
  - [9] G. Thiamova, Y. Grachev, M. Abolghasem, P. Alexa, P.-G. Reinhard, T. R. Rodríguez, and G. S. Simpson, *Phys. Rev. C* **98**, 064304 (2018).
  - [10] P. Hosmer, H. Schatz, A. Aprahamian, O. Arndt, R. R. C. Clement, A. Estrade, K. Farouqi, K.-L. Kratz, S. N. Liddick, A. F. Lisetskiy, P. F. Mantica, P. Möller, W. F. Mueller, F. Montes, A. C. Morton, M. Ouellette, E. Pellegrini, J. Pereira, B. Pfeiffer, P. Reeder, P. Santi, M. Steiner, A. Stolz, B. E. Tomlin, W. B. Walters, and A. Wöhr, *Phys. Rev. C* **82**, 025806 (2010).
  - [11] P. Bączyk, W. Urban, D. Złotowska, M. Czerwiński, T. Rząca-Urban, A. Blanc, M. Jentschel, P. Mutti, U. Köster, T. Soldner, G. de France, G. Simpson, and C. A. Ur, *Phys. Rev. C* **91**, 047302 (2015).
  - [12] B. M. Nyakó, J. Timár, M. Csatlós, Zs. Dombrádi, A. Krasznahorkay, I. Kuti, D. Sohler, T. G. Tornyi, M. Czerwiński, T. Rząca-Urban, W. Urban, P. Bączyk, L. Atanasova, D. L. Balabanski, K. Sieja, A. Blanc, M. Jentschel, U. Köster, P. Mutti, T. Soldner, G. de France, G. S. Simpson, and C. A. Ur, *J. Phys.: Conf. Ser.* **724**, 012051 (2016).
  - [13] A. Astier, M.-G. Porquet, Ts. Venkova, G. Duchene, F. Azaiez, D. Curien, I. Deloncle, O. Dorvaux, B. J. P. Gall, N. Redon, M. Rousseau, and O. Stézowski, *Phys. Rev. C* **88**, 024321 (2013).
  - [14] T. Eronen, V. S. Kolhinen, V.-V. Elomaa, D. Gorelov, U. Hager, J. Hakala, A. Jokinen, A. Kankainen, P. Karvonen, S. Kopecky, I. D. Moore, H. Penttilä, S. Rahaman, S. Rinta-Antila, J. Rissanen, A. Saastamoinen, J. Szerypo, C. Weber f, and J. Äystö, *Eur. Phys. J A* **48**, 46 (2012).
  - [15] I. D. Moore, T. Eronen, D. Gorelov, J. Hakala, A. Jokinen, A. Kankainen, V. S. Kolhinen, J. Koponen, H. Penttilä, I. Pohjalainen, M. Reponen, J. Rissanen, A. Saastamoinen, S. Rinta-Antila, V. Sonnenschein, and J. Äystö, *Nucl. Instrum. Methods Phys. Res. B* **317**, 208 (2013).



- [16] P. Karvonen, H. Penttilä, J. Äystö, J. Billowes, P. Campbell, V.-V. Elomaa, U. Hager, J. Hakala, A. Jokinen, T. Kessler, A. Kankainen, I. D. Moore, K. Peräjärvi, S. Rahaman, S. Rinta-Antila, J. Rissanen, J. Ronkainen, A. Saastamoinen, T. Sonoda, B. Tordoff, and C. Weber, *Nucl. Instrum. Methods Phys. Res. B* **266**, 4454 (2008).
- [17] A. Nieminen, J. Huikari, A. Jokinen, J. Äystö, P. Campbell, and E. C. A. Cochrane, *Nucl. Instrum. Methods Phys. Res. A* **469**, 244 (2001).
- [18] V. S. Kolhinen, T. Eronen, D. Gorelov, J. Hakala, A. Jokinen, K. Jokiranta, A. Kankainen, M. Koikkalainen, J. Koponen, H. Kulmala, M. Lantz, A. Mattera, I. D. Moore, H. Penttilä, T. Pikkarainen, I. Pohjlainen, M. Reponen, S. Rinta-Antila, J. Rissanen, C. Rodríguez Triguero, K. Rytönen, A. Saastamoinen, A. Solders, V. Sonnenschein, and J. Äystö, *Nucl. Instrum. Methods Phys. Res. B* **317**, 506 (2013).
- [19] G. Savard, St. Becker, G. Bollen, H.-J. Kluge, R. B. Moore, Th. Otto, L. Schweikhard, H. Stolzenberg, and U. Wiess, *Phys. Lett. A* **158**, 247 (1991).
- [20] M. Zendel, N. Trautmann, and G. Herrmann, *J. Inorg. Nucl. Chem.* **42**, 1387 (1980).
- [21] S. Raman, B. Fogelberg, J. A. Harvey, R. L. Macklin, P. H. Stelson, A. Schröder, and K.-L. Kratz, *Phys. Rev. C* **28**, 602 (1983).
- [22] BRICC code, <http://bricc.anu.edu.au/>.
- [23] N. B. Gove and M. J. Martin, *At. Data Nucl. Data Tables* **10**, 205 (1971).
- [24] J. Lin, K. Rengan, and R. A. Meyer, *Radiochem. Radioanal. Lett.* **50**, 399 (1982).
- [25] T. D. Johnson and W. D. Kulp, *Nucl. Data Sheets* **129**, 11 (2015).
- [26] M.-G. Porquet, Ts. Venkova, A. Astier, I. Deloncle, A. Prévost, F. Azaiez, A. Buta, D. Curien, O. Dorvaux, G. Duchêne, B. J. P. Gall, F. Khalfallah, I. Piqueras, M. Rousseau, M. Meyer, N. Redon, O. Stézowski, R. Lucas, and A. Bogachev, *Eur. Phys. J. A* **28**, 153 (2006).
- [27] M. Czerwinski, Ph.D. thesis, University of Warsaw, 2017.
- [28] J. C. Hardy, L. C. Carraz, B. Jonson, and P. G. Hansen, *Phys. Lett. B* **71**, 307 (1977).
- [29] I. N. Gratchev, G. S. Simpson, G. Thiamova, M. Ramdhane, K. Sieja, A. Blanc, M. Jentschel, U. Köster, P. Mutti, T. Soldner, G. de France, C. A. Ur, and W. Urban, *Phys. Rev. C* **95**, 051302(R) (2017).
- [30] V. Paar, *Nucl. Phys. A* **211**, 29 (1973); *Phys. Lett. B* **39**, 587 (1972).
- [31] A. Kuriyama, T. Maromuri, and K. Matsuyanagi, *Prog. Theor. Phys.* **47**, 498 (1972); **51**, 779 (1974).
- [32] A. Kuriyama, T. Maromuri, K. Matsuyanagi, and R. Okamoto, *Prog. Theor. Phys.* **53**, 489 (1975).
- [33] K. Sieja, T. R. Rodriguez, K. Kolos, and D. Verney, *Phys. Rev. C* **88**, 034327 (2013).
- [34] P.-G. Reinhard and E. W. Otten, *Nucl. Phys. A* **420**, 173 (1984).
- [35] NNDC database, <https://www.nndc.bnl.gov>.
- [36] K. Sieja, F. Nowacki, K. Langanke, and G. Martínez-Pinedo, *Phys. Rev. C* **79**, 064310 (2009).
- [37] E. Caurier, G. Martínez-Pinedo, F. Nowack, A. Poves, and A. P. Zuker, *Rev. Mod. Phys.* **77**, 427 (2005).
- [38] W. Urban, K. Sieja, T. Materna, M. Czerwiński, T. Rząca-Urban, A. Blanc, M. Jentschel, P. Mutti, U. Köster, T. Soldner, G. de France, G. S. Simpson, C. A. Ur, C. Bernards, C. Fransen, J. Jolie, J.-M. Regis, T. Thomas, and N. Warr, *Phys. Rev. C* **94**, 044328 (2016).
- [39] L. Olivier, S. Franchoo, M. Niikura, Z. Vajta, D. Sohler, P. Doornenbal, A. Obertelli, Y. Tsunoda, T. Otsuka, G. Authalet, H. Baba, D. Calvet, F. Château, A. Corsi, A. Delbart, J.-M. Gheller, A. Gillibert, T. Isobe, V. Lapoux, M. Matsushita *et al.*, *Phys. Rev. Lett.* **119**, 192501 (2017).